

# HiPIMS optimization using mixed high-power and low-power pulsing

H. Eliasson<sup>1</sup>

<sup>1</sup>*Plasma and Coatings Physics Division, Institute of Chemistry,  
Physics and Biology (IFM), Linköpings Universitet,  
Linköping University, SE-581 83 Linköping, Sweden*

(Dated: January 18, 2021)

High-power impulse magnetron sputtering (HiPIMS) is a physical vapor deposition (PVD) technique used for thin film deposition that combines magnetron sputtering with pulsed power technology. The main drawback of HiPIMS is that the deposition rate of the method is lower than for other similar PVD techniques such as direct current magnetron sputtering (dcMS). The main benefit of HiPIMS is a larger ionized flux fraction than other techniques can achieve. It can reach 70-90% compared to just a few percent in dcMS. With short HiPIMS pulses the technique has been shown to reach acceptable deposition rates ( $\sim 70\%$  of dcMS), but at the cost of a lower ionized flux fraction due to lower peak current densities. A way to keep a high peak current density for short pulses ( $2.5\text{--}20\ \mu\text{s}$ ) could be with the addition of pre-ionization. In this study the pre-ionization pulse width and the delay before the HiPIMS pulse was investigated to try and find an optimal set of parameters to maximize the peak current. For our specific experimental setup the optimal pulse length of the pre-ionized pulse was found to be  $20\ \mu\text{s}$ , and the best delay was  $0\ \mu\text{s}$ . From this the conclusion can be drawn that pre-ionization may positively affect the peak current densities in a HiPIMS pulse and that there exists a set of optimal parameters for that said pre-ionization.

## I. INTRODUCTION

Magnetron sputtering is a physical vapor deposition (PVD) technique widely used for the deposition of thin films. In magnetron sputtering a plasma discharge is maintained by applying a constant voltage to the target (cathode). The plasma will be confined close to the target due to the magnetron being placed directly above the target due to the magnetron being placed directly above the target[1].

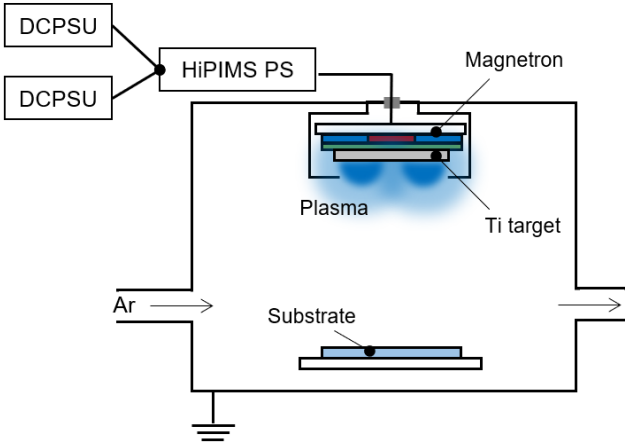


FIG. 1: A cross section of the sputtering chamber. The two DCPSU:s are DC-units and the HiPIMS PS is the pulsing unit.

The basic idea of a magnetron sputtering setup is the following. The chamber is filled with a working gas like argon to start and maintain the plasma discharge. When a plasma is ignited, Ar ions from the plasma will bombard the surface of the target with high enough energy to knock target atoms out into the chamber, referred to as

sputtering, where many things can happen to the target atoms. One of which is that it lands on the substrate and contributes to thin film growth. But it can also get lost to the walls, get ionized in the plasma, or get back attracted to the target again.

In 1999 Kouznetsov et al.[2] introduced High-power impulse magnetron sputtering (HiPIMS), which is the technique that was used in this study. HiPIMS combines magnetron sputtering with pulsed power technology to achieve larger peak currents at a lower duty factor compared to regular direct current magnetron sputtering (dcMS) at the same average target power [1]. It is important not to have a too large average target power since it can cause damage to and/or melting of the target[3]. The main advantage of HiPIMS is a larger ionized flux fraction than other techniques can achieve. It can reach 70-90% compared to just a few percent in dcMS. It is favorable to ionize as large a fraction as possible of the sputtered target atoms. A high ionization flux fraction has many benefits in thin film deposition. Studies have shown that it can lead to the growth of smooth and dense films, enhance mechanical and optical properties as well as enabling uniform films on complex-shaped substrates[4]. The much larger peak current densities achieved in HiPIMS have been found to be correlated with larger ionization flux fractions [1, 4]. For instance Lundin et al[5] have shown that the ionized flux fraction of Ti increased from 20% to 68% as the peak current density increased from  $0.7\text{--}2.5\ \text{A cm}^{-2}$ .

The major drawback of HiPIMS is that HiPIMS has a lower deposition rate than dcMS (usually about 30–80% [6]), meaning that the thin film growth is slower. This drawback is most commonly explained by back-attraction of target ions to the target followed by self-sputtering[1, 7].

For short pulses it has been shown by Konstantini-

dis et al.[8] that the deposition rate can be increased to  $\sim 70\%$  of the value in dcMS. For short pulses however, the peak current will be lower since the current will not have time to reach it's maximum value before the voltage pulse is turned off again. The problem is how to reach an equally high peak current also for short HiPIMS pulses since that means maintaining a high ionized flux fraction also for short pulses.

One way of increasing the current is by the addition of pre-ionization. In other words, trying to change the characteristics of the current waveform by applying a low power pulse before the main HiPIMS pulse. This low power pulse would provide a seed charge to ensure a faster rise of the discharge current in the HiPIMS pulse[9–11]. Although pre-ionization is not a new concept in the field[12], there has not been much research put into optimizing the pre-ionization.

This study focuses on finding an optimal length of the pre-ionization pulse and delay between the pre-ionization pulse and the HiPIMS pulse to maximize the peak current.

## II. EXPERIMENTAL DETAILS

The study was divided into two parts. First a study of the delay time between the pre-ionization pulse and the HiPIMS pulse. Then, using the delay time that yielded the highest peak current, a study of the optimal pre-ionization pulse width was conducted. It is also important to keep the sputter power in the pre-ionization pulse as low as possible, since that stage will only contribute with sputtered neutrals and very few ions. To make sure that the power during the pre-ionization pulse was not too large, the power was also calculated and taken into account when deciding on the optimal pre-ionization pulse width.

All of the experiments were conducted with the same setup. The sputtering chamber was a cylindrical vacuum chamber, 44 cm in diameter and 75 cm high. The magnetron was mounted on the top circular flange of the chamber, facing downwards. The sputtering target was a thick 2"  $\varnothing$  Ti-target mounted on the magnetron. The thickness of the target was 5.6 mm. A 1 mm thick Al spacer was mounted between the target and the magnetron making the total distance between the magnetron and the target surface 6.6 mm. The spacer was added to weaken the magnetic field at the target.

The pulses were controlled by a prototype multi-level HiPIMS pulsing unit capable of generating the desired pre-ionization pulse followed by a regular HiPIMS pulse. Two DC units were connected to that pulser, one to supply the pre-ionization pulse voltage, and the other for the HiPIMS pulse voltage.

The base pressure of the sputtering chamber was kept at around  $10^{-6}$  Torr by a turbomolecular pump. The chamber was filled with argon gas with a purity of 99.9997% through a leak valve connected to the chamber.

For all of the experiments, the pressure in the chamber was kept at 0.5 Pa. A typical current and voltage waveform in a pre-ionized HiPIMS pulse can be seen in Figure 2.

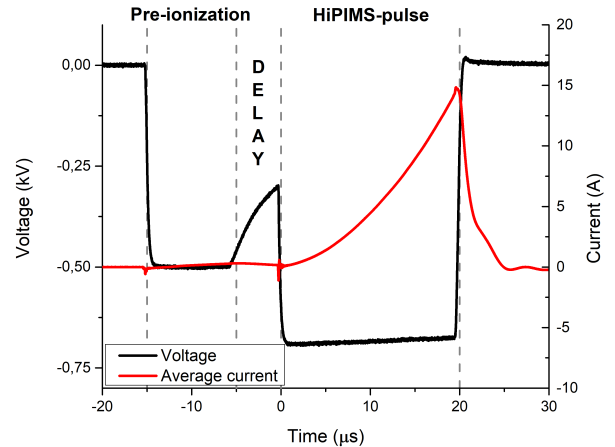


FIG. 2: A typical current and voltage waveform in a pre-ionized HiPIMS pulse. In this case 10  $\mu\text{s}$  of pre-ionization was applied before a 5  $\mu\text{s}$  delay followed by a 20  $\mu\text{s}$  HiPIMS pulse.

The waveforms were later plotted and analyzed. The key features that were analyzed were: the current rise, the power share between the two pulses and the peak current. The current rise was analyzed by looking at the derivative of the different current waveforms at a given current level. The power fraction was calculated by integrating the product of the current and voltage during the pre-ionization and HiPIMS pulse and comparing their individual contributions.

## III. RESULTS

### A. Delay time study

A 5  $\mu\text{s}$  long pre-ionization pulse and a 20  $\mu\text{s}$  long HiPIMS pulse was used in this study. Measurements were done at three different delay times: 1, 5 and 10  $\mu\text{s}$ . The voltage of the HiPIMS pulse was 700 V and the pre-ionization pulse voltage was 550 V. The frequency of the pulses were set to 800 Hz. The voltage and the current waveforms were then measured and averaged over 200 waveforms by a PicoScope oscilloscope with 14-bit resolution.

The results showed that the peak current (denoted  $I_{D,pk}$ ) is increasing the more you decrease the delay between the pre-ionization pulse and the HiPIMS pulse. The delay time which yielded the largest peak current was the delay of 1  $\mu\text{s}$ . The current and voltage waveforms of that measurement is displayed in Figure 3. A comparison between all

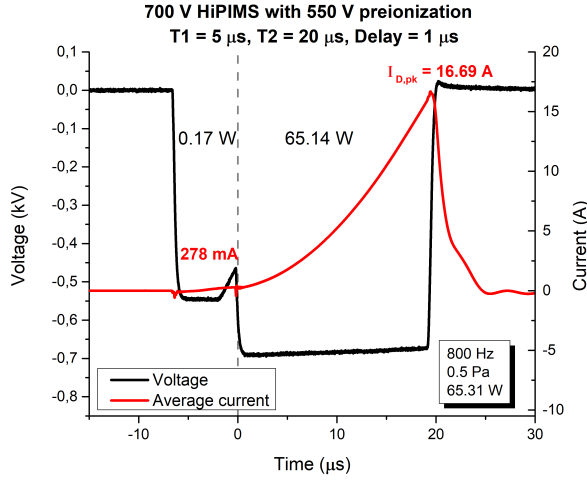


FIG. 3: Current and voltage waveforms for the measurement that yielded the highest peak current in study IIIA. T1 is the pre-ionization pulse width and T2 is the HiPIMS pulse width. The peak current  $I_{D,pk}$  was measured to 16.69 A

of the current waveforms in the delay time study is compiled in Figure 4. Added to the comparison is also a measurement without any pre-ionization. The pre-ionization increased the peak current for all of the tested delay times.

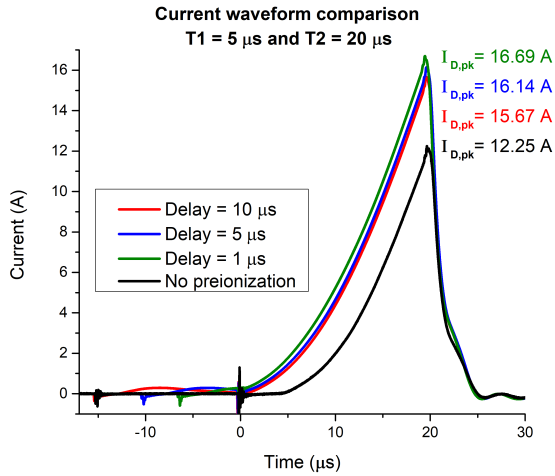


FIG. 4: The current waveforms of different delays compared with each other and with a case of no pre-ionization. T1 is the pre-ionization pulse width and T2 is the HiPIMS pulse width.

It is also apparent from Figure 4 that without pre-ionization, the current rise starts much later than in the cases with pre-ionization. The time between the applied HiPIMS voltage pulse and a noticeable rise in the current changes with pre-ionization. We call this the time-lag of the current waveform. So pre-ionization seems to reduce time-lag.

The characteristics of the current waveforms in Figure 4 are quite similar except for the observable time-lag. This implies that the current rate increase remained the same independent of delay time. So it seems as the delay length has little to no impact on the derivatives of the current curves. Therefore the derivatives were not calculated in this study.

The power fraction of the pre-ionization pulse with a delay of 1  $\mu$ s (FIG. 3) was 0.26%. For the measurements with 5  $\mu$ s delay and 10  $\mu$ s delay, the power fraction was 0.78% and 0.99% respectively. The peak currents also decreased with increasing delays. For the 1  $\mu$ s delay the peak current was 16.69 A and for the 5  $\mu$ s and 10  $\mu$ s delay the peak currents were 16.14 A and 15.67 A respectively.

## B. Pulse length study

Using the results from the previous study, six pre-ionization pulse widths were tested, keeping the delay time constant. These pulse widths were investigated: 5  $\mu$ s, 10  $\mu$ s, 20  $\mu$ s, 30  $\mu$ s, 40  $\mu$ s, 50  $\mu$ s. The delay times used were 1  $\mu$ s and 0  $\mu$ s. The voltage of the 20  $\mu$ s HiPIMS pulse was 700 V and the pre-ionization pulse voltage was 550 V. The frequency of the pulses were set to 800 Hz. The voltage and the current waveforms were then measured and averaged over 200 waveforms by a PicoScope oscilloscope with 14-bit resolution.

In this study, the combination that yielded the largest peak current was the one with 20  $\mu$ s pre-ionization and a 0  $\mu$ s delay (Figure 5). The measured peak current  $I_{D,pk}$  was 17.75 A.

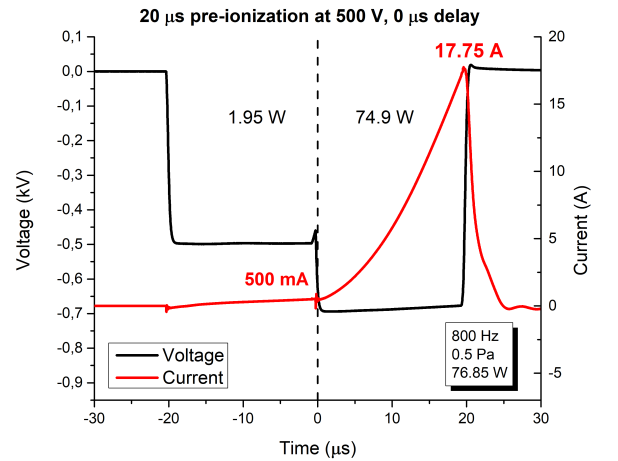


FIG. 5: Current and voltage waveforms for the measurement that yielded the highest peak current in study IIIB. T1 is the pre-ionization pulse width and T2 is the HiPIMS pulse width. The peak current  $I_{D,pk}$  was measured to 17.75 A

A comparison between the current waveforms in this study can be found in Figure 6. An interesting observation is that there seems to be an optimum around 20  $\mu$ s

for the pre-ionization pulse width, which I will get back to in the discussion. All of the pre-ionization pulse current waveforms were not included in the comparison. This was because the graph got very crowded. The omitted pulse widths (10  $\mu\text{s}$ , 30  $\mu\text{s}$  and 50  $\mu\text{s}$ ) followed the same pattern as the ones in the figure but showed little promise of maximizing the peak current. All the measured peak currents are instead displayed in FIG. 7 where the optimum at 20  $\mu\text{s}$  is clearly visible.

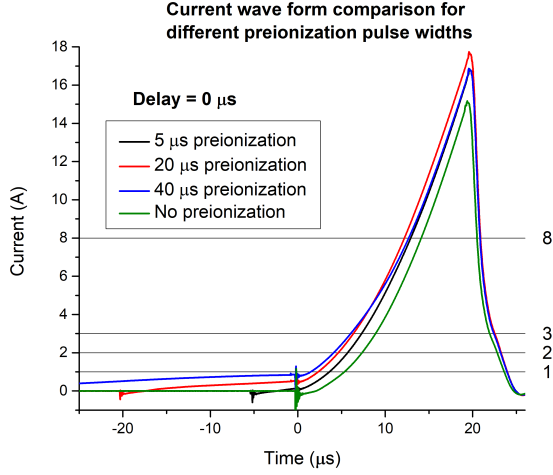


FIG. 6: A comparison of the HiPIMS discharge current waveforms in study III B. The maximum HiPIMS peak current is reached for the case with 20  $\mu\text{s}$  pre-ionization. The characteristics of the waveforms differ. The current values 8 A, 3 A, 2 A and 1 A are levels chosen to display a difference in the derivative of the curves.

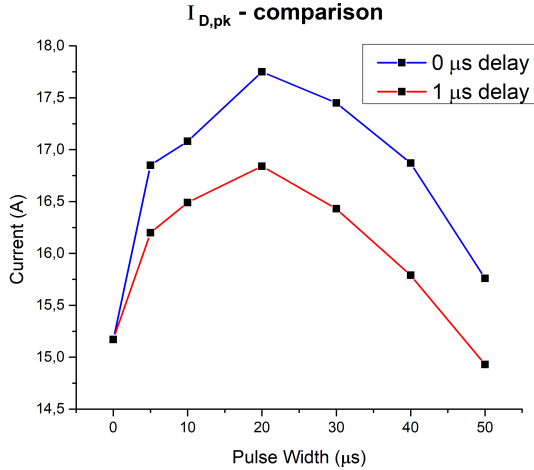


FIG. 7: All of the measured peak currents in Study III B. There is a clear maximum at 20  $\mu\text{s}$  for both delay times.

In contrast to study III A, the current waveforms in this study look quite different to each other. The derivatives of the current curves at the values specified in Figure

6 reveal that the case of no pre-ionization is actually the curve which rises the fastest out of all the curves. Due to the time-lag however, it ends up being the curve with the lowest peak current. The trend is visualized in Figure 8 below. At 8 A the HiPIMS pulse without pre-ionization was rising with a slope of 1.16 A/ $\mu\text{s}$ . All the calculated derivatives are following the same decreasing trend for longer pre-ionization pulse widths, except for one. The case of 20  $\mu\text{s}$  pre-ionization at 8 A is rising faster than the 5  $\mu\text{s}$  and 10  $\mu\text{s}$  pulses at the same current value.

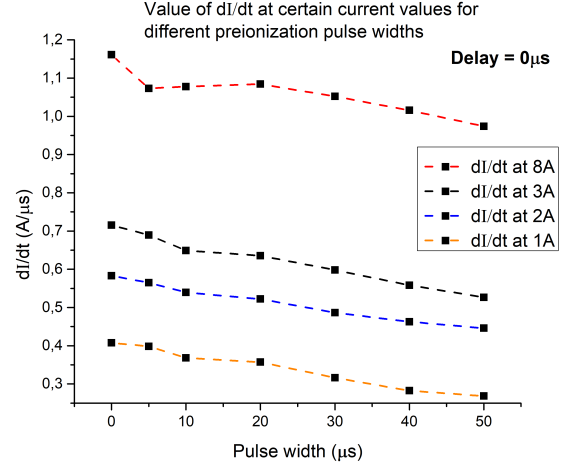


FIG. 8: The values of the current waveforms' derivatives at 8 A, 3 A, 2 A and 1 A.

If the derivatives at all these current levels were the same for the different current waveforms, then the change in peak current would only be due to time-lag. This may have been the case in FIG. 4. But FIG. 8 confirms that the current waveforms are indeed different in this study.

Another result to note is that the pre-ionization increases the peak current of the system in almost all cases in both study III A and III B. The only measurements where the addition of pre-ionization lowered the peak current was with a 1  $\mu\text{s}$  delay and a pre-ionization pulse width of 50  $\mu\text{s}$  (FIG. 7).

How large a portion of the total power in the system that was contributed by the pre-ionization pulse has been calculated and compiled in Table I below. The trend shows that smaller pre-ionization pulse widths correspond to a lower contribution to the total power of the pulse.

Delay \ PPW	5 $\mu$ s	10 $\mu$ s	20 $\mu$ s	30 $\mu$ s	40 $\mu$ s	50 $\mu$ s
0 $\mu$ s	X	0.54%	2.5%	5.6%	9.4%	14%
1 $\mu$ s	0.06%	0.8%	3.1%	6.6%	10.8%	15.5%

TABLE I: The fraction of the total power contributed by the pre-ionization pulse. The value marked with X could not be calculated but considering the pattern we can assume it to be smaller than 0.06% (PPW = Pre-ionization pulse width)

#### IV. DISCUSSION

The results suggest that for a given setup, there exists a combination of a pre-ionization pulse width and a delay time that maximizes the peak current density in a pre-ionized HiPIMS pulse. For this specific setup, those values seem to be around 20  $\mu$ s for the pre-ionization pulse and a 0  $\mu$ s delay. It is however likely that these values are only optimal for the specific setup used in this study. How the optimal values change, if they do, based on the setup is for future research to decide. Based on this idea I believe that the value 20  $\mu$ s should not be given too much attention. Instead the realisation that there seems to be an optimum is what should be focused on.

The addition of a delay between the two pulses seems to not be beneficial in terms of maximizing the peak current density. This probably has to do with the built-up seed charge from the pre-ionization pulse decaying during the delay. The variation in seed charge densities may be what is causing the differences in the current waveforms shown in FIG. 6. With longer delays we also saw the power fraction of the pre-ionization pulse grow larger. This I believe was due to two reasons. The first one being that the delay was counted as part of the pre-ionization pulse. The integral of the delay is not zero as can be seen in FIG. 3 and will therefore add to the power. The second reason is that the peak currents were smaller for longer delays. Since the HiPIMS pulse contributes much more to the total power than the pre-ionization pulse, this reduces the total power in the system and thus the power fraction of the pre-ionization pulse will be larger.

Why the peak current is lower for longer delays in Study III A is an interesting question. We also saw something similar in study III B, but then it was longer pre-ionization pulses that reduced the peak current. This could be due to gas rarefaction, that too much of the working gas was ionized before the main HiPIMS pulse. As a consequence of gas rarefaction there would be less gas to ionize during the HiPIMS pulse, leading to lower

currents since there are fewer charge carriers.

There is a clear result showing in both FIG. 4 and FIG. 6, and that is that the pre-ionization increased the peak current within the HiPIMS pulse. This indicates that the addition of pre-ionization may increase the ionization flux fraction of the operation. It is also important to note that it increased the pre-ionization pulse without contributing a lot to the total power, at least for the lower pulse lengths of 5  $\mu$ s, 10  $\mu$ s and 20  $\mu$ s. It is important that the average power across the target is not too high due to risk of melting or causing damage to the magnetron.

A way to expand upon this work would be to investigate the deposition rates and the ionized flux fractions of discharges with the optimal parameters discovered in this study. This would be interesting to compare with the ionized flux fraction and deposition rate of an identical HiPIMS pulse but without pre-ionization. In this way it could be understood if these optimal parameters, in terms of peak current density, actually translate into a larger ionized flux fraction and a higher deposition rate. This would pave the way for a dedicated study on how to increase the deposition rate in HiPIMS using the here-proposed short HiPIMS pulse lengths at maintained, or even higher, ionized flux fractions.

Another direction for future research could be to repeat the experiment for different target sizes, target materials, and background gases to see if any relation can be found between those parameters and the optimal pre-ionization pulse length.

#### V. CONCLUSIONS

From this study the conclusion can be drawn that, for some setups, there exists an optimal pre-ionization pulse width for maximizing the peak current density of a pre-ionized HiPIMS pulse. Further research must be done to determine if this maximized peak current actually translates to a higher ionized flux fraction and an increased deposition rate. That would imply that the addition of a pre-ionization pulse with the right parameters to a HiPIMS pulse could improve its performance in many applications.

Another important conclusion is that pre-ionization, if done right, can greatly improve the aquired peak current density of a HiPIMS pulse. It can do this while keeping the power of the pre-ionization pulse low, so that it only contributes a few percent(2-5%) to the total power of the operation.

- 
- [1] D. Lundin and K. Sarakinos, Journal of Materials Research **27**, 780 (2012).
  - [2] V. Kouznetsov, K. Macák, J. M. Schneider, U. Helmersson, and I. Petrov, Surface and Coatings Technology **122**,

290 (1999).

- [3] D. Lundin, The HiPIMS Process, Ph. D. thesis (2010).
- [4] A. Butler, N. Brenning, M. A. Raadu, J. T. Gudmundsson, T. Minea, and D. Lundin, Plasma Sources Science

- and Technology **27**, 105005 (2018).
- [5] D. Lundin, M. Čada, and Z. Hubička, Plasma Sources Sci. Technol. **24**, 035018 (2015).
  - [6] M. Samuelsson, D. Lundin, J. Jensen, M. A. Raadu, J. T. Gudmundsson, and U. Helmersson, Surface and Coatings Technology **205**, 591 (2010).
  - [7] D. Christie, Journal of Vacuum Science Technology A - J VAC SCI TECHNOL A **23**, 330 (2005).
  - [8] Konstantinidis, Stephanos, Dauchot, J. Pierre, M. Ganciu, A. Ricard, and M. Hecq, Journal of Applied Physics **99**, 013307 (2006).
  - [9] M. Ganciu, S. Konstantinidis, Y. Paint, J. P. Dauchot, M. Hecq, L. de Poucques, P. Vašina, M. Meško, J. C. Imbert, J. Bretagne, et al., Optoelectron. Adv. M **7**, 2481 (2005).
  - [10] P. Poolcharuansin, B. Liebig, and J. Bradley, IEEE T Plasma Sci **38**, 3007 (2010).
  - [11] P. Vašina, M. Meško, J. C. Imbert, M. Ganciu, C. Boisse-Laporte, L. de Poucques, M. Touzeau, D. Pagnon, and J. Bretagne, Plasma Sources Sci. Technol. **16**, 501 (2007).
  - [12] D. V. Mozgrin, High-current low-pressure quasi-stationary discharge in a magnetic field: Experimental research Ph. D. thesis (1994).